Yersiniabactin contributes to overcoming zinc restriction during *Yersinia pestis* infection of mammalian and insect hosts

Sarah L. Price[a] , Viveka Vadyvaloo[b] , Jennifer K. DeMarco[c], Amanda Brady[a] , Phoenix A. Gray[a] , Thomas E. Kehl-Fie[d], Sylvie Garneau-Tsodikova[e] , Robert D. Perry[f], and Matthew B. Lawrenz[a,c,1]

[a]Department of Microbiology and Immunology, University of Louisville School of Medicine, Louisville, KY 40202; [b]Paul G. Allen School for Global Health, Washington State University, Pullman, WA 99164; [c]Center for Predictive Medicine for Biodefense and Emerging Infectious Diseases, University of Louisville, Louisville, KY 40292; [d]Department of Microbiology and Carl R. Woese Institute for Genomic Biology, University of Illinois Urbana–Champaign, Champaign, IL 61820; [e]Department of Pharmaceutical Sciences, University of Kentucky College of Pharmacy, Lexington, KY 40536; and [f]Department of Microbiology, Immunology, and Molecular Genetics, University of Kentucky School of Medicine, Lexington, KY 40506

Yersinia pestis causes human plague and colonizes both a mammalian host and a flea vector during its transmission cycle. A key barrier to bacterial infection is the host's ability to actively sequester key biometals (e.g., iron, zinc, and manganese) required for bacterial growth. This is referred to as nutritional immunity. Mechanisms to overcome nutritional immunity are essential virulence factors for bacterial pathogens. *Y. pestis* produces an iron-scavenging siderophore called yersiniabactin (Ybt) that is required to overcome iron-mediated nutritional immunity and cause lethal infection. Recently, Ybt has been shown to bind to zinc, and in the absence of the zinc transporter ZnuABC, Ybt improves *Y. pestis* growth in zinc-limited medium. These data suggest that, in addition to iron acquisition, Ybt may also contribute to overcoming zinc-mediated nutritional immunity. To test this hypothesis, we used a mouse model defective in iron-mediated nutritional immunity to demonstrate that Ybt contributes to virulence in an iron-independent manner. Furthermore, using a combination of bacterial mutants and mice defective in zinc-mediated nutritional immunity, we identified calprotectin as the primary barrier for *Y. pestis* to acquire zinc during infection and that *Y. pestis* uses Ybt to compete with calprotectin for zinc. Finally, we discovered that *Y. pestis* encounters zinc limitation within the flea midgut, and Ybt contributes to overcoming this limitation. Together, these results demonstrate that Ybt is a bona fide zinc acquisition mechanism used by *Y. pestis* to surmount zinc limitation during the infection of both the mammalian and insect hosts.

siderophores | nutritional immunity | *Yersinia pestis* and plague | zinc acquisition | insect vectors

The gram-negative bacterium *Yersinia pestis* is a reemerging pathogen that causes bubonic, septicemic, and pneumonic plague in humans. *Y. pestis* is a zoonotic pathogen maintained in the environment in rodent populations across the globe and is transmitted within these populations by a flea vector (1–4). As such, the bacterium has evolved specific factors that contribute to the colonization of both its mammalian and insect hosts (1, 2). Human bubonic plague manifests from the bite of an infected flea. After deposition into the dermis by the flea, *Y. pestis* disseminates to and colonizes the draining lymph nodes, resulting in the development of an inflamed lymph node referred to as a bubo. Septicemic plague occurs when bacteria are directly inoculated into blood vessels by fleas or when bacteria disseminate from the lymph node to the bloodstream during bubonic plague. Via the blood, *Y. pestis* can spread to other tissues, including the lungs, in which infection can progress to the development of secondary pneumonic plague. The aerosolization of the bacteria from the lungs by coughing can further lead to person-to-person transmission, causing primary pneumonic plague in naïve individuals (1, 5, 6). Without timely treatment, all three forms of plague are associated with high-mortality rates. Because of the possibility for direct human-to-human transmission, the lack of a Food and Drug Adminstration (FDA)-approved vaccine, and the potential for weaponization, *Y. pestis* is also considered a bioterrorism threat (7). Therefore, understanding the pathogenesis of *Y. pestis* will help in the development of potential therapeutic approaches to protect against both environmental and man-made threats by *Y. pestis*.

Transition metals are essential nutrients required for proper cellular function, which makes them a crucial component for biological processes in all forms of life. Bacteria require transition metals in order to maintain intermediary metabolism, transcriptional regulation, and virulence for bacterial pathogens (8–11). Since transition metals are vital for bacterial proliferation and infection, eukaryotic hosts sequester these essential nutrients from invading pathogens via a mechanism referred to as nutritional immunity (8, 12, 13). Nutritional immunity includes both tightly controlling systemic metal concentrations via the regulation of metal absorption from the diet and local restriction in response to infection through the

Significance

Transition metals are required for proper cellular function, which renders them critical for all life. To restrict bacterial infection, eukaryotic organisms actively sequester these transition metals, a concept referred to as nutritional immunity. Consequently, bacterial pathogens have evolved dedicated mechanisms to acquire transition metals in order to colonize the host. During human plague, *Yersinia pestis* overcomes iron limitation via the production of the secreted siderophore yersiniabactin. Here, we identify an iron-independent role for yersiniabactin in evading zinc-mediated nutritional immunity during mammalian infection and in *Y. pestis* colonization of the flea–insect vector. Importantly, yersiniabactin is found in several pathogens, indicating that a variety of bacteria use it to acquire multiple metals in order to overcome nutritional immunity.

release of metal-binding proteins by innate immune cells (11, 14). For example, neutrophils responding to infection can release a variety of metal-binding proteins via both degranulation and formation of neutrophil extracellular traps (NETs) to restrict metal access by bacterial and fungal pathogens (15–17). Calprotectin is one of these metal-binding proteins and is a heterodimer composed of two S100 family members, S100A8 and S100A9 (18–22). Via two metal binding sites, calprotectin is able to restrict microorganism access to manganese (Mn), zinc (Zn), and iron (Fe) (19, 23–26). Zn sequestration by calprotectin has been shown to be a major barrier to the colonization by several bacterial pathogens, including *Salmonella* Typhimurium, *Clostridioides difficile*, *Staphylococcus aureus*, *Acinetobacter baumannii*, and some strains of *Helicobacter pylori* (26–31).
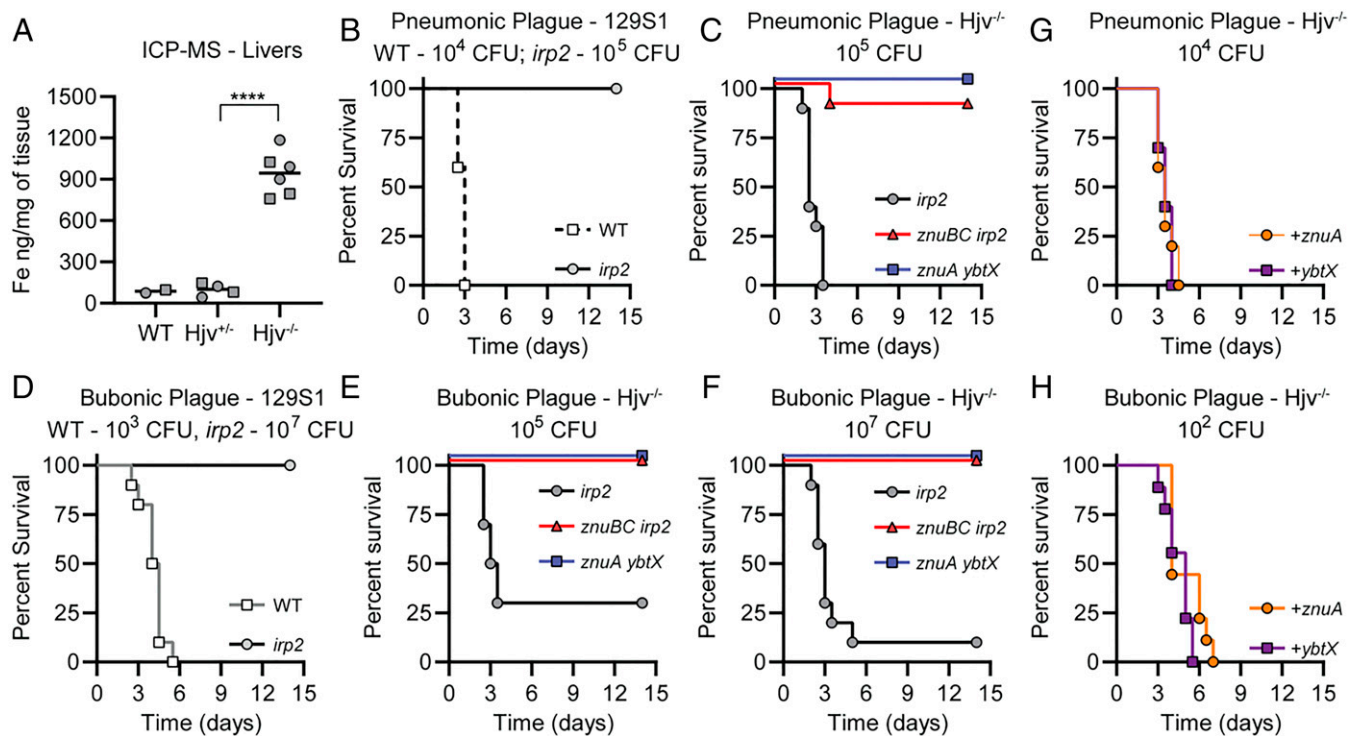
To overcome nutritional immunity, pathogens have evolved a variety of dedicated mechanisms to acquire transition metals during infection (14), and siderophores are some of the most robust mechanisms used by bacteria to specifically overcome host-mediated Fe limitation (32, 33). Yersiniabactin (Ybt) represents one class of siderophore used by *Yersinia* species, *Klebsiella pneumoniae*, pathogenic *Escherichia coli*, and other enteric pathogens to colonize the mammalian host (33–39). In *Y. pestis*, the synthesis and import machinery for Ybt are encoded on a high-pathogenicity genomic island within the *pgm* locus on the chromosome (40, 41). Ybt is synthesized by the Ybt synthetase complex consisting of YbtE, YbtT, YbtU, HMWP1, and HWMP2, and it is exported by the bacterium through an unknown mechanism (41, 42). Ybt binds to ferric Fe with a formation constant of 4×10^{36}, allowing it to outcompete host nutritional immunity Fe-binding proteins such as lactoferrin and transferrin (43, 44). Once bound to Fe, Ybt-Fe is recognized by the outer membrane receptor Psn and imported across the outer membrane in a TonB-dependent manner (45). YbtP and YbtQ are then responsible for the import of the Ybt-Fe complex across the inner membrane (46). The importance of Ybt-mediated Fe acquisition to virulence has been demonstrated for *Yersinia*, *Klebsiella*, and *E. coli* by generating mutations in both the Ybt synthesis and import machinery (36, 44, 47, 48). For *Y. pestis* specifically, Ybt mutants are significantly attenuated for growth in Fe-limited medium in vitro and in causing lethal infection in both bubonic and pneumonic plague models (44).

While originally described as an Fe-scavenging molecule, several recent studies indicate that Ybt can bind to other transition metals, suggesting that Ybt may also be used for the acquisition of metals other than Fe. Using purified Ybt and liquid chromatography mass spectrometry, Koh et al. showed that Ybt can bind several divalent transition metals, including nickel (Ni) and copper (Cu) (49). The same group later showed that *E. coli* can use Ybt to acquire Cu and Ni during metal limitation and may also use Ybt to protect against Cu toxicity when Cu is present in excess (50, 51). Using a native spray metabolomics approach validated by NMR, Zhi et al. demonstrated that Ybt can also bind to Zn and that the expression of Ybt by the probiotic bacterium *E. coli* Nissle 1917 contributes to a selective advantage over *S. enterica* Typhimurium under Zn-limited conditions, including within the inflamed gut (52). A role for Ybt in Zn acquisition has been further supported by previous studies in *Y. pestis*. Specifically, while a *Y. pestis* mutant lacking the Zn importer ZnuABC is partially attenuated for in vitro growth in Zn-limited medium, a *znuBC irp2* mutant (*irp2* encodes the HMWP2 Ybt synthetase) is significantly more attenuated for growth in the same medium (53, 54). Moreover, the *znuBC irp2* mutant is attenuated in the septicemic plague model, a model in which *znuBC* and *irp2* are not individually required for virulence (54). Finally, Bobrov et al. also discovered that Ybt-dependent growth in Zn-limited medium does not require the Ybt-Fe transport machinery (Psn, TonB, YbtP, and YbtQ) in *Y. pestis* but instead requires the YbtX inner membrane protein (54, 55). The role of YbtX in Ybt-dependent Zn acquisition has been subsequently confirmed in *E. coli* Nissle 1917 (52). Together, these data strongly support a hypothesis that Ybt not only contributes to the acquisition of Fe but also Zn, and possibly other metals, during *Y. pestis* infection. Here, we test this hypothesis and demonstrate that Ybt contributes to *Y. pestis* virulence in the mammalian host independent of Fe acquisition. Furthermore, we show that *Y. pestis* uses the ZnuABC and Ybt Zn acquisition systems to colonize the flea–insect vector and to overcome calprotectin-mediated nutritional immunity during mammalian infection.

Results

Ybt Contributes to *Y. pestis* Virulence Independent of Fe Acquisition in the Mammalian Host. A *Y. pestis* mutant lacking the Zn transporter ZnuABC (denoted as *znuBC*; this mutant is a deletion of *znuC*, *znuB*, and the promoter region for *znuA*) and the ability to make Ybt (a deletion of *irp2*) is significantly more attenuated than *znuBC* or *irp2* single mutants in the mouse model of septicemic plague (54), suggesting that Ybt contributes to Zn acquisition in vivo. However, because Ybt is also essential for Fe acquisition in vivo (44), the infection of wild-type (WT) mouse models does not rule out the possibility that the *znuBC irp2* phenotype is an additive effect of limited Zn acquisition due to the inactivation of *znuABC* and limited Fe acquisition due to the inactivation of *irp2*. Therefore, to expand on these previous studies and more directly test the role of Ybt in Zn acquisition in vivo, we chose a mouse model of plague in which host-imposed Fe limitation is not a barrier to *Y. pestis* infection. Hemojuvelin-deficient mice (Hjv$^{-/-}$) are unable to properly maintain Fe homeostasis, resulting in the increased absorption of Fe from their diet and accumulation of Fe within their tissues but not the accumulation of other metals (Fig. 1*A* and *SI Appendix*, Table S1) (56). Importantly, Quenee et al. previously showed that Hjv$^{-/-}$ mice are susceptible to infection by *Y. pestis* that have lost the pigmentation genetic locus (*pgm*) and are subsequently unable to produce Ybt, further demonstrating that Fe-mediated nutritional immunity is not a barrier to *Y. pestis* in this model (57). We confirmed that attenuation was specific for the loss of Ybt by demonstrating that parent 129S1 mice are resistant to infection by an *irp2* mutant (Fig. 1 *B* and *D*), while Hjv$^{-/-}$ mice are sensitive to infection (Fig. 1 *C*, *E*, and *F*). Therefore, the infection of Hjv$^{-/-}$ mice should allow us to separate the role of Ybt in Fe acquisition from Zn acquisition in virulence. Toward this end, Hjv$^{-/-}$ mice were challenged intranasally with 10^5 colony forming units (CFU) of the *znuBC irp2* mutant. While 100% of Hjv$^{-/-}$ mice infected with the *irp2* mutant succumbed to infection within 3.5 d (Fig. 1*C*), only one mouse from two independent studies (*n* = 10) developed a lethal infection when challenged with the *znuBC irp2* mutant (*P* < 0.0001). To determine if the route of infection impacted survival, separate groups of animals were challenged subcutaneously with 10^5 CFU of bacteria. In this model of bubonic plague, 70% of Hjv$^{-/-}$ mice succumbed to infection with the *irp2* mutant, while all mice survived infection with the *znuBC irp2* mutant (Fig. 1*E*; *P* < 0.0001). When the challenge dose was increased to 10^7 CFU, mortality increased to 90% for the *irp2* mutant, but still, none of the mice infected with the *znuBC irp2* mutant developed a lethal infection (Fig. 1*F*; *P* < 0. 0001). To further show that Ybt-dependent Zn acquisition is responsible for the attenuated phenotype, we generated an independent mutant in the *znuABC* system by deleting the *znuA* gene, which encodes the periplasmic, substrate-binding component of the system, and the *ybtX* gene, which encodes a membrane permease that we showed previously is required for Ybt-dependent Zn acquisition in vitro but not Ybt-dependent

Price et al.
Yersiniabactin contributes to overcoming zinc restriction during *Yersinia pestis* infection
of mammals and fleas

Fig. 1. Ybt contributes to virulence independent of Fe. (*A*) Fe concentrations of livers from C57BL/6J (WT), Hjv$^{-/+}$, or Hjv$^{-/-}$ mice, as determined by ICP-MS. Male mice are represented by squares and female mice by circles. Unpaired two-tailed *t* test, ****$P < 0.0001$. (*B*) 129S1 mice were challenged intranasally with indicated inoculum of *Y. pestis* (WT; white squares) or *irp2* mutant (gray circles) and monitored every 12 h for the development of moribund disease for 14 d. (*C*) Hjv$^{-/-}$ mice were challenged intranasally with the indicated inoculum of *irp2* (gray circles), *znuBC irp2* (red triangles), or *znuA ybtX* (blue squares) mutants and monitored every 12 h for the development of moribund disease for 14 d. (*D*) 129S1 mice were challenged subcutaneously with the indicated inoculum of *Y. pestis* (WT, white squares) or *irp2* mutant (gray circles) and monitored every 12 h for the development of moribund disease for 14 d. (*E* and *F*) Hjv$^{-/-}$ mice were challenged subcutaneously with the indicated inocula of *irp2* (gray circles), *znuBC irp2* (red triangles), or *znuA ybtX* (blue squares) mutants and monitored every 12 h for the development of moribund disease for 14 d. (*G* and *H*) Hjv$^{-/-}$ mice were challenged with the indicated inoculum of the *znuA ybtX* mutant complemented with *ybtX* (purple squares) or the *znuA ybtX* mutant complemented with *znuA* (orange circles) and monitored every 12 h for the development of moribund disease for 14 d. Results are the combined data from two independent experiments (*n* = 10 total).

Fe acquisition (55). When Hjv$^{-/-}$ mice were challenged with 10^5 CFU of the *znuA ybtX* mutant intranasally, all mice survived the 14-d infection period (Fig. 1*C*; $P < 0.0001$). This attenuated phenotype was also observed in the bubonic plague model, even when mice were challenged with 10^7 CFU (Fig. 1 *E* and *F*; $P < 0.0001$). Importantly, the genetic complementation of *znuA ybtX* with an intact copy of the *ybtX* or *znuA* genes restored the virulence of the mutant (Fig. 1 *G* and *H*). Of note, mice infected with the *znuBC irp2* or *znuA ybtX* mutants that survived to the end of these studies did not have any detectable bacteria present within their spleens, livers, or lungs. Collectively, these data demonstrate that Ybt contributes to infection independent of Fe acquisition and support the hypothesis that ZnuABC and Ybt are redundant Zn acquisition systems important for mammalian infection.

Y. pestis Colonization of the Flea Vector Requires ZnuABC and Ybt Zn Acquisition Systems. Despite the importance of the flea vector in *Y. pestis* transmission, metal availability in the flea midgut has been minimally characterized (58). Since the *znuA ybtX* mutant is extremely attenuated in its ability to grow in Zn-limited environments, and YbtX is not required for Ybt-mediated Fe acquisition, this mutant provides us a tool to specifically investigate the availability of Zn within the flea midgut and to determine the role of Zn transporters in flea colonization by *Y. pestis*. To this end, *Xenopsylla cheopis* fleas were coinfected using an artificial feeder system, as previously described (59, 60), with a mixture of *Y. pestis* carrying a kanamycin (Kan)

resistance marker (designated as WT) and *Y. pestis* with mutations in the *znuABC* and Ybt Zn acquisition systems and lacking the Kan marker [all strains lacked the pCD1 virulence plasmid that is not required for flea colonization (59)]. Around 2 h after feeding, a subset of fleas was euthanized, and bacteria were enumerated by replica plating on brain heart infusion (BHI) agar with and without Kan to determine the ratio of the WT *Y. pestis* to the mutant bacteria initially ingested by the fleas during the blood meal. At 7- and 14-d postinfection, bacteria were enumerated from fleas in the same fashion to determine if the mutants had a fitness defect, which would be indicated by an increase in the percentage of recovered WT *Y. pestis* (*SI Appendix*, Fig. S1). During coinfections with WT *Y. pestis* and either the *znuBC* or *ybtX* mutants, no fitness advantage was observed in the parental strain (Fig. 2 *A* and *B*). However, when fleas were coinfected with WT *Y. pestis* and the *znuA ybtX* double mutant, significantly more WT bacteria were isolated from the fleas than mutant bacteria by 14-d postinfection compared to day 0 postinfection in two independent experiments (Fig. 2 *C* and *D*; $P < 0.01$ and $P < 0.001$, respectively). Together, these data demonstrate that the ZnuABC and Ybt Zn acquisition systems provide a fitness advantage to *Y. pestis* during flea colonization and suggest that Zn availability is limited within the midgut of the flea.

Y. pestis Induces Host Calprotectin Expression during Infection. The inability of the *znuBC irp2* and *znuA ybtX* mutants to infect Swiss Webster (55) and Hjv$^{-/-}$ (Fig. 1) mice indicates that

www.manaraa.com
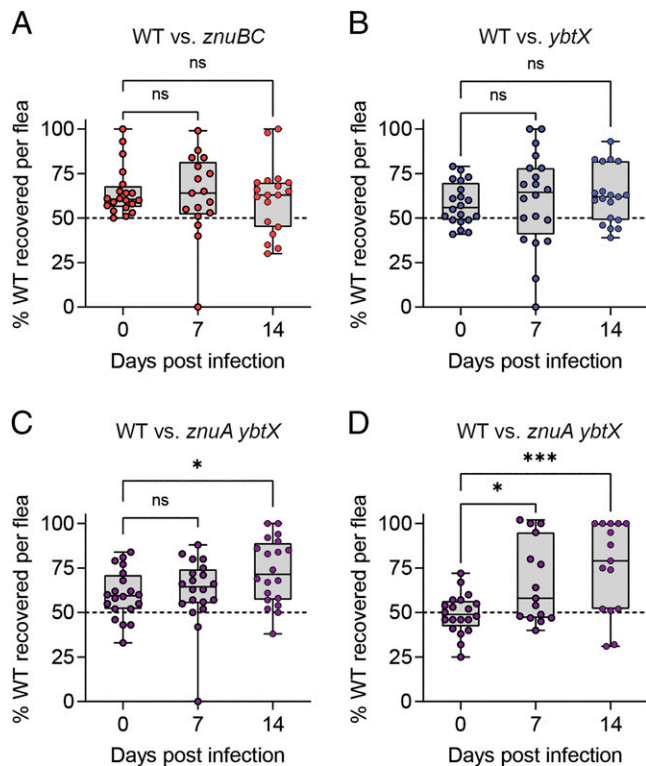
Fig. 2. Mutants deficient in Zn acquisition are less fit to colonize the flea vector. *X. cheopis* fleas were infected using an artificial feeder with a mixture of *Y. pestis glmS-pstS*::kan^R (designated as WT) and Zn acquisition mutants. At indicated time points, bacteria were enumerated, and the ratio of WT to mutant bacteria was calculated for WT versus *znuBC* (A), WT versus *ybtX* (B), or WT versus *znuA ybtX* (C and D). Greater recovery of WT at days 7 or 14 indicates that the mutant bacteria are less fit to colonize the flea. Each point represents bacterial enumeration from an individual flea; fleas in which infection was not established were excluded (*n* = 15 to 20). One-way ANOVA with Dunnett's compared to day 0; ns = not significant, *$P \leq 0.05$ and ***$P \leq 0.001$. C and D represent biologically independent replicate experiments.

Y. pestis encounters Zn restriction during infection. One of the primary mechanisms used by the host to sequester Zn is through the release of calprotectin by neutrophils and other host cells at sites of infection (17). Comer et al. previously reported an increase in the transcription of S100A8 and S100A9 (the subunits comprising calprotectin) in the lymph nodes of rats infected with *Y. pestis* (61). To confirm that *Y. pestis* also encounters calprotectin during infection of mice, C57BL/6J mice were subcutaneously infected with *Y. pestis*, and the transcription of several host nutritional immunity proteins within the draining lymph nodes was measured (Fig. 3*A*). The transcription of the siderophore-binding protein lipocalin 2 [which binds enterobactin but not Ybt (62)] and the Fe-binding proteins haptoglobin and lactoferrin increased within 36-h postinfection. However, we did not observe the increased transcription of transferrin in the lymph nodes. The increased transcription of S100A8 and S100A9 was observed by 48-h postinfection. To determine if calprotectin is encountered by *Y. pestis* during pneumonic plague, C57BL/6J mice were infected intranasally with *Y. pestis*, and extracellular calprotectin was measured in the bronchial alveolar lavage fluid (BALF) over the first 48 h of infection (Fig. 3*B*). Compared to the mock, infected mice, significantly more extracellular calprotectin was recovered in *Y. pestis*–infected BALF at 24- and 48-h postinfection ($P < 0.01$ and $P < 0.0001$, respectively). Together, these data confirm that calprotectin is present within *Y. pestis*–infected tissues during both bubonic and pneumonic plague.

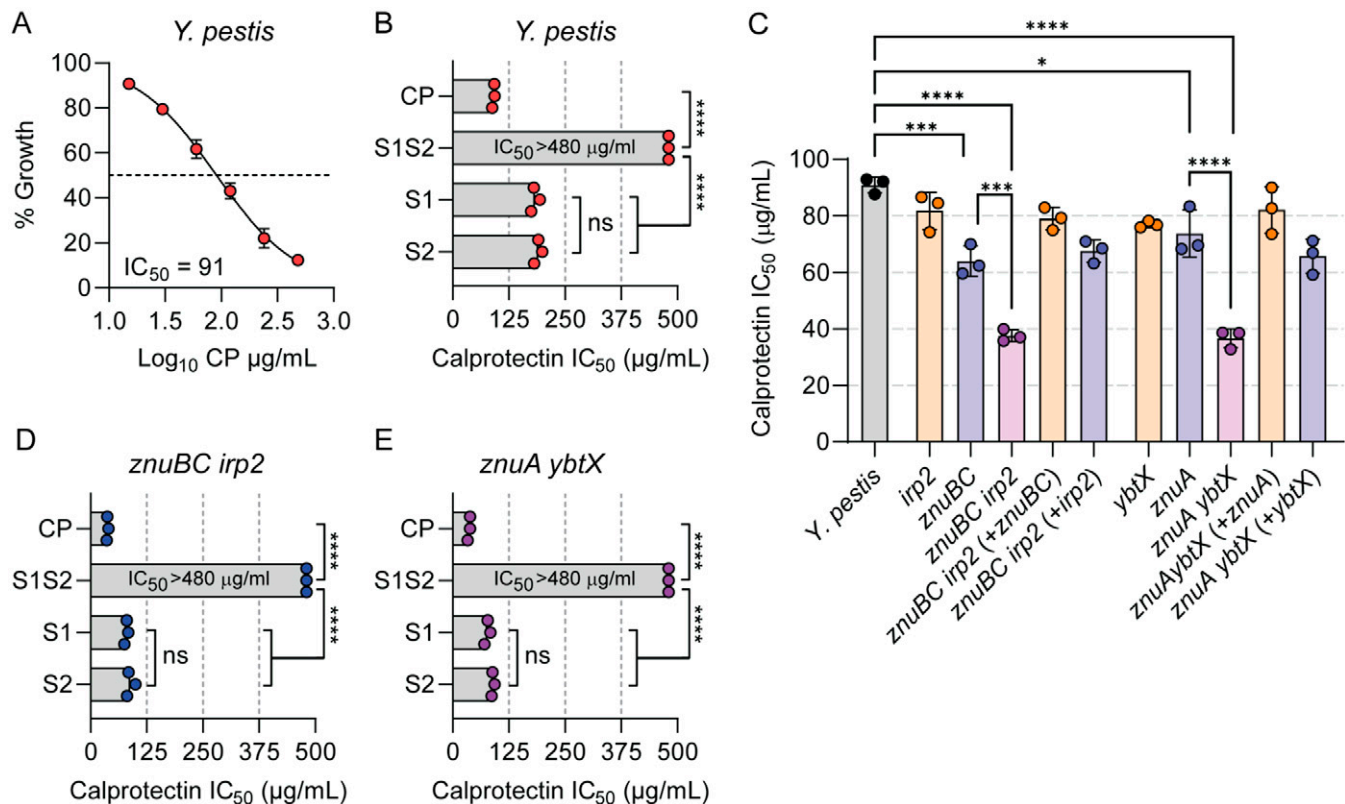**Zn Sequestration by Calprotectin Restricts the Growth of *Y. pestis*.** Since our in vivo data indicated that *Y. pestis* encounters calprotectin during infection, we next asked if calprotectin could restrict the growth of *Y. pestis*. *Y. pestis* lacking the pCD1 plasmid and carrying the pGEN-*luxCDABE*–luminescent bioreporter (63) (designated as WT *Y. pestis*) was incubated in BHI with increasing concentrations of recombinant calprotectin, and bacterial growth as a function of the bioluminescence produced by pGEN-*luxCDABE* was kinetically monitored for 8 h (63) to calculate the concentration of calprotectin that inhibited bacterial growth in BHI by 50% (IC_{50}). A dose-dependent inhibition of WT *Y. pestis* growth was observed, revealing an IC_{50} of 91 (±5) μg/mL of calprotectin in BHI (Fig. 4*A*). To determine if the calprotectin-mediated restriction of *Y. pestis* growth is dependent on metal sequestration, WT *Y. pestis* was incubated with recombinant calprotectin inactivated for metal binding. Calprotectin has two metal binding sites designated Site 1 (S1; six His site) and Site 2 (S2; three His Asp site) (25, 26). S1 binds multiple metals, including Mn, Zn, and Fe (20, 26), while S2 binds to Zn but not Mn or Fe (64, 65). The inactivation of both metal binding sites eliminated the ability of calprotectin to inhibit *Y. pestis* growth at the highest concentration of calprotectin tested (Fig. 4*B*; $IC_{50} > 480$ μg/mL; $P \leq 0.0001$), supporting that the calprotectin restriction of *Y. pestis* growth is due to metal sequestration. To determine the contribution of specific metal sequestration by calprotectin on growth, WT *Y. pestis* was incubated with recombinant calprotectin mutated in only one of the metal binding sites. The inactivation of only the S1 Mn/Zn/Fe binding site increased the IC_{50} of calprotectin by approximately twofold, compared to WT calprotectin [Fig. 4*B*; $IC_{50} = 182$ (±9) μg/mL; $P \leq 0.0001$]. A similar approximately twofold increase in the IC_{50} was observed when the bacteria were incubated with calprotectin mutated only for the S2 Zn only binding site [Fig. 4*B*; $IC_{50} = 190$ (±9) μg/mL; $P \leq 0.0001$]. Moreover, the IC_{50} of the S1 mutant, which cannot bind Mn or Fe but can sequester Zn, is not statistically different that the S2 mutant, which can sequester all three metals, indicating that calprotectin Zn sequestration is sufficient to restrict *Y. pestis* growth under these conditions.

ZnuABC and Ybt Improve the Ability of *Y. pestis* to Grow in the Presence of Calprotectin. Since calprotectin Zn sequestration appears to restrict the growth of *Y. pestis*, we next determined whether ZnuABC or Ybt improves the ability of *Y. pestis* to grow in the presence of calprotectin. While significantly lower concentrations of calprotectin were required to inhibit the
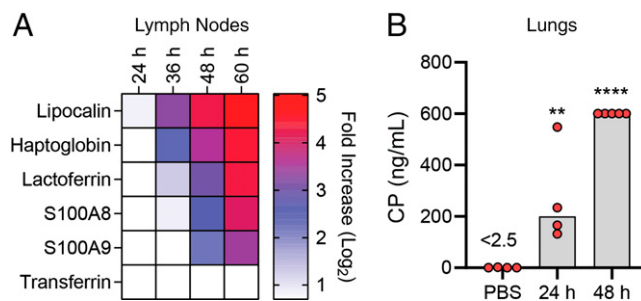
Fig. 3. *Y. pestis* induces calprotectin expression during infection. (*A*) C57BL/6J mice were infected subcutaneously with *Y. pestis*, and draining lymph nodes were harvested at indicated time points (*n* = 5) for RNA isolation and transcription analysis by microarray. Data are shown as transcriptional fold-change in infected tissues compared to lymph nodes from uninfected mice. (*B*) C57BL/6J mice were instilled with *Y. pestis* or PBS by intranasal installation, BALF was collected at 24 and 48 h, and extracellular calprotectin (CP) was measured. Each point represents an individual mouse, and bars represent the mean. One-way ANOVA with Dunnett's compared to PBS control: **$P \leq 0.01$ and ****$P \leq 0.0001$. For *B*, data are representative of two independent experiments.

Fig. 4. ZnuABC and Ybt both contribute to overcoming Zn sequestration by calprotectin. (*A*) WT *Y. pestis* was incubated with increasing concentrations of calprotectin (CP), up to 480 µg/mL, and percent growth versus untreated was determined at 8 h to calculate the IC_{50}. (*B*) IC_{50} of calprotectin-containing mutations in metal binding Site 1 (S1), metal binding Site 2 (S2), or both metal binding sites (S1S2) when incubated with WT *Y. pestis*. (*C*) IC_{50} of calprotectin when incubated with indicated *Y. pestis* mutants. Complete statistical comparisons between all bacteria for *C* is in *SI Appendix*, Table S2. (*D* and *E*) IC_{50} of calprotectin-containing mutations in metal binding S1, metal binding S2, or S1S2 when incubated with *znuBC irp2* (*D*) or *znuA ybtX* (*E*) mutants. For *B*, *D*, and *E*, the S1S2 mutant was unable to inhibit *Y. pestis* growth at the highest concentration tested (480 µg/mL). Each point represents the mean IC_{50} of a biologically independent experiment ($n = 3$), and the bar represents the mean of the three independent experiments. One-way ANOVA with Tukey's comparison: ns = not significant; *$P < 0.05$; ***$P < 0.001$; and ****$P < 0.0001$.

growth of the *znuBC* and *znuA* mutants compared to WT *Y. pestis* [Fig. 4*C*; $IC_{50} = 64$ (± 10) µg/mL; $P \leq 0.001$; and $IC_{50} = 73$ (± 15) µg/mL; $P \leq 0.05$, respectively], the growth of the *irp2* and *ybtX* mutants in the presence of calprotectin was not significantly different from WT *Y. pestis*. However, strains lacking both Zn acquisition systems (*znuBC irp2* or *znuA ybtX*) had significantly greater growth defects than the single mutants (Fig. 4*C*; $P \leq 0.0001$). The complementation of the double mutants with genes from either Zn acquisition system restored the ability of the double mutant to grow in the presence of calprotectin (Fig. 4*C* and *SI Appendix*, Table S2). The inactivation of either metal binding site in calprotectin resulted in an approximate twofold increase in the IC_{50} of calprotectin when incubated with the *znuBC irp2* or *znuA ybtX* mutants ($P \leq 0.0001$), but no significant differences were observed in the IC_{50} of the S1 and S2 mutant forms of calprotectin (Fig. 4 *D* and *E*). Together, these data support that ZnuABC and Ybt are redundant Zn acquisition systems that improve the ability of *Y. pestis* to evade Zn-mediated growth restriction by host calprotectin.

Calprotectin Is the Primary Zn Sequestration Barrier to Infection by *Y. pestis*. Because *Y. pestis* appears to encounter calprotectin during infection, we next asked if calprotectin is a barrier to *Y. pestis* during mammalian infection. $S100A9^{-/-}$ mice, which lack one of the subunits that compose calprotectin (66), or C57BL/6J mice (the parental background for the $S100A9^{-/-}$ mice) were infected either intranasally (10^5 CFU) or subcutaneously (10^3 CFU) with either WT *Y. pestis* or the *znuA ybtX* mutant (which

is attenuated for Zn acquisition but not Fe acquisition and for growth in the presence of calprotectin in vitro). Surprisingly, we did not observe any statistically significant differences in the kinetics of lethal infection by WT *Y. pestis* in the $S100A9^{-/-}$ mice compared to C57BL/6J mice, as measured by log-rank test, in either the pneumonic (Fig. 5*A*; $P = 0.1462$) or bubonic (Fig. 5*B*; $P = 0.556$) plague models, indicating that WT *Y. pestis* efficiently overcomes calprotectin metal restriction. However, while the *znuA ybtX* mutant was completely attenuated in C57BL/6J mice, virulence was restored in $S100A9^{-/-}$ mice, with the kinetics of lethal infection in the $S100A9^{-/-}$ mice similar to WT *Y. pestis* infection. These data demonstrate that calprotectin represents a nutritional barrier to *Y. pestis* during both pneumonic and bubonic plague and that *Y. pestis* encodes two Zn acquisition systems, ZnuABC and Ybt, to overcome Zn sequestration mediated by calprotectin and to cause lethal infection.

Discussion

Siderophores are essential for the virulence of a variety of pathogens (32, 67). Because of their high affinity for Fe, their role in virulence has been primarily linked to the improved competition for Fe with host nutritional immunity mechanisms. However, while in vitro data indicates that siderophores can also bind metals other than Fe, the contribution of alternative metal binding by siderophores to virulence has been largely overlooked. In the case of Ybt, several independent groups have shown recently that Ybt can bind to Ga, Ni, Cu, Cr, and Zn and, to a lesser degree, Co, Pd, Mg, and Al in addition to

www.manaraa.com
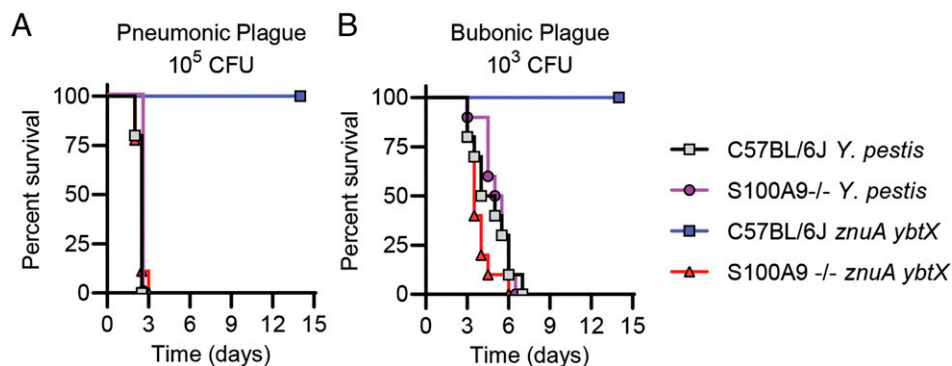
Fig. 5. Calprotectin is the primary barrier to infection by the *znuA ybtX* mutant. (*A*) C57BL/6J or S100A9$^{-/-}$ mice were infected intranasally with 10^5 CFU of WT *Y. pestis* or the *znuA ybtX* mutant. (*B*) C57BL/6J or S100A9$^{-/-}$ mice were infected subcutaneously with 10^3 CFU of WT *Y. pestis* or the *znuA ybtX* mutant. Results are the combined data from two independent experiments (*n* = 10 total). Log-rank test revealed no significant differences in survival kinetics between S100A9$^{-/-}$ mice infected with WT *Y. pestis* or the *znuA ybtX* mutant or C57BL/6J and S100A9$^{-/-}$ infected with WT *Y. pestis*.

Fe (49, 52, 68–71). Moreover, Ybt has been shown to improve the in vitro growth of *E. coli* in Cu-, Ni-, or Zn-limited media (50–52) and of *Y. pestis* in Zn-limited medium (54). However, direct evidence for a role of alternative metal binding by Ybt in virulence has been difficult to demonstrate for two reasons. First, many pathogens encode redundant metal acquisition systems that can mask the contribution of Ybt to metal acquisition. For example, several pathogens that encode Ybt also encode the high-affinity ZnuABC Zn transporter, which has been shown to compensate for growth defects under Zn limitation in the absence of Ybt in both *Y. pestis* and *E. coli* Nissle 1917 (52, 55). Second, for those pathogens that express Ybt, Ybt is the primary Fe acquisition system during infection, which makes it difficult to separate Fe-dependent contributions from other metal-dependent contributions to overall virulence. To overcome these hurdles, we used a combination of *Y. pestis* Ybt mutants lacking the ZnuABC Zn acquisition system and the Hjv$^{-/-}$ mouse strain defective in Fe-mediated nutritional immunity to clearly demonstrate in vivo that Ybt contributes to the virulence of *Y. pestis* independent of Fe acquisition. These data build upon the in vitro data by others (49–55) and support the concept that Ybt should be considered more than a siderophore and likely better described as a metallophore that can contribute to the acquisition of multiple metals during *Y. pestis* infection. Moreover, because Ybt and the Ybt transporter YbtX are conserved in other pathogenic bacteria, these data suggest that Ybt likely contributes to the pathogenic potential for a variety of bacteria through an increased ability during infection to scavenge not only Fe but also Zn and possibly other metals. This hypothesis is further supported by the improved competition of *E. coli* Nissle 1917 expressing Ybt over *S. enterica* Typhimurium in the Zn-limited environment of the inflamed gut recently reported by Zhi et al. (52). Furthermore, the potential to increase the ability of bacterial pathogens to compete against multiple arms of the host nutritional immunity response during infection may also help to explain the hypervirulent phenotypes associated with *K. pneumoniae* clinical isolates that harbor the Ybt genetic loci (72–75). The application of similar strategies described here for *Y. pestis* in these other bacteria could be used to determine the contribution of alternative metal acquisition by Ybt to the hypervirulence observed in certain clinical isolates that has been associated with the presence of the Ybt genetic loci.

While metal restriction has been established as an important barrier to bacterial infection in the mammalian host, a role for metal sequestration in restricting the bacterial colonization of insect vectors has not been established. However, homologs of mammalian, Fe-binding transferrins have been identified in several insects (76), and in a *Drosophila melanogaster* model system, transferrin 1 sequesters Fe and facilitates nutritional immunity to

Pseudomonas aeruginosa (77), suggesting the possible conservation of metal nutritional immunity in insects. Previous studies have shown that Ybt is not required for the flea colonization by *Y. pestis* (78, 79) and that Fe is not limited in the flea midgut (58). In contrast, we show here that the *znuA ybtX* mutant, which can acquire Fe but not Zn, is significantly attenuated in flea colonization (Fig. 2). These data support the hypothesis that bacterial access to Zn is limited within the flea midgut but requires future biochemical analysis to directly determine the availability of Zn in flea gut tissue. Whether the flea is actively restricting Zn is not known. However, the first flea genome was recently published (80) and provides a resource that may lead to the identification of potential nutritional immunity genes that could contribute to Zn limitation, based on homology with mammalian genes. Alternatively, *Y. pestis* may need high-affinity Zn acquisition systems to compete for Zn with members of the microbiota of the flea digestive tract. How the microbiota of the flea effects the transmission of *Y. pestis* has not been investigated, but similar to the mammalian host, it is likely the microbiota imposes selective pressures on pathogens that use these insects for transmission. Regardless of the mechanism for Zn limitation, these data demonstrate a role for Zn acquisition systems as transmission factors for *Y. pestis* and justify future studies to better understand metal restriction within fleas and other insects and the potential impact of these systems on pathogen transmission.

Recently, a role for YezP in Zn transport has been suggested in *Yersinia pseudotuberculosis* (81–83). YezP is secreted by the type VI secretion system cluster four (T6SS-4), can bind Zn, and a *Y. pseudotuberculosis znuABC yezP* mutant is attenuated in the mouse model of Yersiniosis (81). Furthermore, the T6SS-4 is regulated by ZntR and Zur, which typically regulate genes involved in Zn homeostasis, including ZnuABC and ZntA (82, 83). However, unlike *znuABC* and *zntA*, the regulation of the T6SS-4 genes in *Y. pseudotuberculosis* appears to be independent of Zn availability (82). Furthermore, the T6SS-4 genes in *Y. pseudotuberculosis* and *Y. pestis* are activated by Zur, which normally represses the expression of Zn acquisition systems (82, 84), suggesting that YezP does not play a role in Zn homeostasis. This hypothesis is further supported by our previously published data that a *Y. pestis znuBC y3657* mutant (*y3657* is the YezP homology in *Y. pestis*) is no further attenuated for growth in Zn-limited medium than a *znuBC* mutant (55). Instead, T6SS-4 appears to confer a growth advantage for a *Y. pseudotuberculosis znuABC* mutant in the presence of reactive oxygen species when grown under Zn-limited conditions, leading to the hypothesis that YezP binding to Zn may increase Zn-mediated resistance to reactive oxygen intermediates encountered during infection (81). Whether the T6SS-4 contributes to *Y. pestis* resistance to oxidative stress remains to be explored, but based on all these data, it is unlikely that YezP

and the T6SS-4 system have a significant role in maintaining Zn homeostasis during the *Y. pestis* infection of the mammalian host. Interestingly, a whole-genome transcriptional study by Chouikha et al. comparing gene expression during flea infection between *Y. pestis* and a *Y. pseudotuberculosis* mutant that is flea transmissible revealed that the T6SS-4 was more highly up-regulated in *Y. pseudotuberculosis* than in *Y. pestis*, while *ybt* genes, including *ybtX*, were more highly up-regulated in *Y. pestis* (85). These data provide additional evidence that Ybt and YbtX, and not YezP and the T6SS-4, contribute to overcoming Zn limitation during *Y. pestis* flea infection.

The mammalian host produces a variety of proteins that can sequester Zn from invading pathogens (12, 13). In the mouse, calprotectin expression and release by host cells has been shown to occur during a variety of bacterial infections (27, 28, 86), and we observed evidence of increased calprotectin levels in *Y. pestis*–infected tissues during plague (Fig. 3). These data suggest that *Y. pestis* needs to overcome calprotectin-mediated nutritional immunity to proliferate in these tissues. This hypothesis is independently supported by observations published by other laboratories. Comer et al. reported a similar increase in S100A8 and S100A9 in the lymph nodes of rats infected with *Y. pestis* (61), and Nuss et al. reported the increased transcription of these genes in the Peyer's patches during the infection of the closely related enteric pathogen *Y. pseudotuberculosis* (87). Despite these previous observations, the role of calprotectin in restricting *Yersinia* infections has not been previously tested directly. Interestingly, the kinetics of lethal infection of S100A9$^{-/-}$ mice with WT *Y. pestis* did not appear to differ from that of C57BL/6J (Fig. 5). This phenotype differs from what has been reported for other pathogens, in which S100A9$^{-/-}$ mice are more susceptible to infection than mice that produce functional calprotectin (27, 28, 30, 86). These data suggest that *Y. pestis* has evolved very effective mechanisms to overcome calprotectin-mediated nutritional immunity, to which the ZnuABC and Ybt systems appear to be the major contributors to overcoming the Zn sequestration by calprotectin. Future studies using the *znuA ybtX* mutant to identify the impact of calprotectin beyond overall host survival, such as monitoring of bacterial dissemination and proliferation in different tissues, will allow us to specifically determine when *Y. pestis* encounters calprotectin-mediated Zn restriction during the progression of plague.

Calprotectin has been shown to sequester Mn, Zn, and Fe from bacterial and fungal pathogens (26–28, 88, 89). Using recombinant forms of calprotectin with different metal-binding abilities suggests that the calprotectin-mediated sequestration of Zn is a barrier for *Y. pestis*, at least under the in vitro conditions in which we tested here. This is supported by the observation that the calprotectin S1 metal binding site mutant, which is ablated for Mn and Fe sequestration but can sequester Zn, was still able to inhibit *Y. pestis* growth compared to the S1S2 mutant (Fig. 4*B*). Studies with other pathogens, such as *S. aureus*, have shown that Mn sequestration by calprotectin is necessary for maximal antimicrobial activity (25, 86), highlighting that the evolution of calprotectin to sequester multiple metals has resulted in a broad-spectrum antimicrobial protein that can restrict the growth of a variety of pathogens that vary in their ability to acquire different metals. Like we have shown for Zn, *Y. pestis* also encodes multiple Mn acquisition systems, including the Yfe and MntH systems (90). In the absence of these Mn transporters, Mn binding via the S1 metal binding site might have a greater impact on growth restriction than observed here. However, a *yfe mntH* mutant is only partially attenuated during bubonic plague and does not appear to be attenuated during pneumonic plague (90), indicating that additional Mn acquisition mechanisms may be active during infection to overcome calprotectin-mediated Mn sequestration. Alternatively, *Y. pestis* may be able to use other metals such as Fe to compensate for Mn restriction during infection, as reported for *Streptococcus pneumoniae* (91).

While we observed an additive effect on the growth of *Y. pestis* in the presence of calprotectin when we inactivated both the Znu and Ybt Zn acquisition systems, the data from the single mutants suggest that the integral membrane ZnuABC transporter may be more effective in scavenging Zn than Ybt in the presence of calprotectin (Fig. 4*C* and *SI Appendix*, Table S2). These data were unexpected, as previous studies with *S. aureus* have shown that staphylopine, a secreted Zn-binding metallophore, is better at scavenging Zn in the presence of calprotectin than AdaABC, a membrane-bound Zn transporter (89). However, these results may be a reflection of Ybt expression by *Y. pestis* in these assays. For these studies, *Y. pestis* was cultured under metal replete conditions prior to incubation with calprotectin. Under these growth conditions, Ybt synthesis is minimal (44, 92). A greater contribution of Ybt may be observed if the bacteria are pregrown under metal deplete conditions to increase the expression of Ybt in the *znuABC* mutants. Alternatively, while ZnuABC is a dedicated Zn transporter, Ybt also binds to Fe and other metals, and thus, binding competition between different metals by Ybt may result in the appearance of a decreased contribution for Zn acquisition in these experiments. Importantly, we have previously shown that absence of the ZnuABC system does not impact virulence (54, 55), demonstrating that in vivo Ybt alone is sufficient to scavenge Zn in the presence of calprotectin.

Because the *znuA ybtX* mutant is not defective in Fe acquisition, this mutant provided us a powerful tool to directly test for the role of calprotectin-mediated Zn restriction during plague. The inactivation of calprotectin by deletion of S100A9 in the host completely restored the virulence of this double mutant (Fig. 5). Moreover, we did not observe a significant difference between the kinetics of the infection with WT or *znuA ybtX* bacteria, indicating that calprotectin is the main barrier to Zn acquisition in mice during bubonic and pneumonic plague. These data also support that calprotectin is a potent barrier to bacteria attempting to colonize the host via intradermal or pulmonary routes. Because S100A8 and S100A9 comprise upwards of 40% of the total cytosolic proteins in neutrophils (93, 94) and neutrophil-mediated calprotectin release has been linked to growth restriction of several pathogens (26, 31, 95), neutrophils tend to be considered the primary cells responsible for the release of calprotectin during infection. However, neutrophil inflammation in response to *Y. pestis* differs dramatically within the initial tissues colonized by *Y. pestis* during bubonic and pneumonic plague. During intradermal infection (bubonic plague), a rapid recruitment of neutrophils is observed to the infection site (79, 96, 97). However, during pulmonary infection (pneumonic plague), the infiltration of neutrophils is delayed (6, 98). These differences in neutrophil recruitment raise the possibility that calprotectin-dependent restriction may be mediated by different cells within different tissues. The role of cells other than neutrophils in mediating calprotectin restriction has been reported in the gut for *S. enterica* Typhimurium and in the dermis for *Borrelia burgdorferi*, another vector-borne bacterium (99, 100), and our future goals are to use the *znuA ybtX* mutant to dissect the contribution of different cell types to the calprotectin response in specific tissues during bubonic and pneumonic plague.

In conclusion, we have directly demonstrated an Fe-independent role of the siderophore Ybt in the *Y. pestis* virulence and colonization of both the mammalian and insect hosts. Because of the conservation of YbtX in enteric pathogens that produce Ybt, we expect that Ybt also contributes to Zn acquisition in other pathogens encoding the Ybt genetic loci. Although Ybt has long been referred to as a siderophore, data from our group and others support the notion that Ybt binds to and improves the acquisition of at least two and, possibly, multiple metals and thus should be considered a bona fide metallophore. Furthermore, these data open the possibility that, as a field, we need to examine whether other siderophores

Price et al.
Yersiniabactin contributes to overcoming zinc restriction during *Yersinia pestis* infection of mammalian and insect hosts

PNAS | **7 of 10**
https://doi.org/10.1073/pnas.2104073118
www.manaraa.com

MICROBIOLOGY

may also contribute to the overall virulence through the acquisition of metals other than Fe.

Methods

Ethics Statement. 129S1, 129S1 Hjv$^{-/-}$ (56), and C57BL/6J were originally purchased from The Jackson Laboratories and bred within the barrier facility at the Clinical and Translational Research Building at the University of Louisville, and C57BL/6J S100A9$^{-/-}$ mice (66) were bred at the University of Illinois at Urbana–Champaign prior to transfer to the University of Louisville for infection. Groups contained both male and female mice, and no sex bias was observed during these studies. Animals were housed in accordance with NIH guidelines, and all procedures were approved by the University of Louisville Institutional Animal Care and Use Committee (IACUC) and the University of Illinois IACUC. Three d prior to challenge with *Y. pestis*, animals were transferred to University of Louisville's Center for Predictive Medicine Regional Biocontainment Animal Biosafety Level-3 (ABSL-3) Laboratory to acclimate to the facility. Mice were maintained within ABSL-3 for up to 14 d postchallenge.

Bacterial Strains and Plasmids. All bacterial mutants in these studies were generated in the *Y. pestis* KIM6+ background [pCD1$^{(-)}$ pMT$^{(+)}$ pPCP1$^{(+)}$ pgm$^{(+)}$] (101) and confirmed by PCR and sequencing. The generation of the *znuBC* and *znuBC irp2* mutants was described in Desrosiers et al. by generating an in-frame deletion of *znuC*, *znuB*, and the entire promoter region for *znuA* and generating an in-frame deletion of *irp2* (41, 53). The generation of the *znuA* and *znuA ybtx* mutant was described by Bobrov et al. by generating in-frame deletions of *znuA* and *ybtX* (41, 54, 55). To ensure that Zn phenotypes were not a result of secondary mutations, complemented mutants were generated by restoring genes at the native sites by homologous recombination using pSR47s (102) and confirmed by PCR, sequencing, and the restoration of growth in Zn-limited medium (*SI Appendix*, Fig. S2). For animal infections, mutant strains were transformed with the pCD1Ap^R plasmid, and pCD1Ap^R, pMT1, pPCP1, and the pgm locus were confirmed by PCR, as previously described (103). In vivo calprotectin measurements were made from animals infected with *Y. pestis* CO92 [pCD1$^{(+)}$ pMT$^{(+)}$ pPCP1$^{(+)}$ pgm$^{(+)}$]. For in vitro calprotectin experiments, strains were transformed with the pGEN-*luxCDABE* plasmid (104) to monitor bacterial growth by bioluminescence, as we have previously described (63), and were grown in the presence of carbenicillin (50 μg/mL). *Y. pestis* was routinely grown for 15 to 18 h at 26 °C in Difco BHI broth (BD Biosciences) with aeration. Prior to pneumonic infection, *Y. pestis* grown at 26 °C was diluted to an optical density at 600 nm of 0.05 in BHI broth with 2.5 mM CaCl$_2$ and grown at 37 °C with aeration for 16 to 18 h (6). Bacterial concentrations were determined using a spectrophotometer and diluted to desired concentrations in 1× phosphate-buffered saline (PBS) for mouse infections or fresh medium for in vitro studies. Concentrations of bacterial inoculums for mouse studies were confirmed by serial dilution and enumeration on agar plates.

Inductively Coupled Plasma Mass Spectrometry. To determine Fe and Zn as well as other metal concentrations in mice, livers were harvested from 8-wk-old mice, and 10 to 20 mg liver tissue was incubated at 65 °C in 70% nitric acid for 4 h and then diluted 35-fold in Milli-Q purified, metal-free water. The solution was passed through a 100-μm filter, and metal levels were measured by inductively coupled plasma mass spectrometry (ICP-MS) (Thermo Fisher Scientific X-Series II) at the University of Louisville's Center for Integrative Environmental Health Science Toxicomics and Environmental Measurement Facility Core. Metal levels were calculated based on a standard curve and presented as nanogram/milligram wet tissue.

Animal Infections with *Y. pestis*. Mice were challenged with *Y. pestis* as previously described (63, 105, 106). Briefly, for intranasal challenge, mice were anesthetized with ketamine/xylazene and administered 20 μL bacteria suspended in 1× PBS to the left nare. For the subcutaneous challenge, mice were anesthetized with isoflurane and administered 20 μL bacteria suspended in 1× PBS via subcutaneous injection at the base of the tail. Infected mice were monitored for the development of disease symptoms twice daily for 14 d. Moribund animals meeting predefined endpoint criteria were humanely euthanized by CO$_2$ asphyxiation and scored as succumbing to infection 12 h later.

Flea Infections with *Y. pestis*. Flea coinfection experiments were conducted as described in methods outlined in Lemon et al. (59). Briefly, separate cohorts of *X. cheopis* fleas were allowed to blood feed on infected sodium heparinized CD-1 mouse blood (BioIVT) using a previously described artificial feeding apparatus (59, 60). The bloodmeal was seeded with a 1:1 ratio of the *Y. pestis* KIM6+ *glmS-pstS*::kan^R strain, and either the *ybtX*, *znuBC*, or *znuA ybtX* mutants to achieve a final concentration of 1.08×10^9 to 1.82×10^9 CFU/mL blood. Only fleas that fed to repletion were selected. Infected fleas were fed maintenance bloodmeals on days 5, 8, and 12 postacquisition of the infected blood meal. At 0-, 7-, and 14-d postinfection, 20 coinfected fleas were processed to enumerate bacterial colonization (*SI Appendix*, Fig. S1). To ensure the optimal growth of the Zn acquisition mutants, agar plates were additionally supplemented with 10 μM ZnCl$_2$. A second independent experiment was completed only for the *znu ybtX* mutant to confirm its aberrant fitness phenotype. Guidelines set forth by the US NIH Guide for the Care and Use of Laboratory Animals (107) and approved by the Washington State University IACUC were strictly applied when using mice in flea infection experiments.

Measurement of Calprotectin during *Y. pestis* Infection. To determine the expression of calprotectin during bubonic plague, C57BL/6J mice were infected subcutaneously with ~200 CFU *Y. pestis*. At 24-, 36-, 48-, and 60-h postinfection, the draining lymph nodes were harvested from five mice. Lymph nodes from each time point were combined, total RNA was extracted, and host transcriptional profiles were determined, as previously described, and compared to lymph nodes from uninfected mice (108). To determine extracellular levels of calprotectin within the lungs during pneumonic plague, mice were infected intranasally with ~10^4 CFU of *Y. pestis*, and at 24- and 48-h postinfection, groups of mice were euthanized, and BALF was collected as previously described (109). Host cells and *Y. pestis* were removed from the samples using a 0.45-μm syringe filter, and total extracellular concentrations of calprotectin were determined using the Mouse Calprotectin SimpleStep ELISA (enzyme-linked immunosorbent assay) Kit, as described by the manufacturer(-Abcam, ab263885).

Determination of Calprotectin Inhibitory Concentrations. Recombinant forms of calprotectin were produced in *E. coli* and purified as previously described (25, 26). To determine the concentrations of calprotectin to inhibit 50% growth of *Y. pestis*, bacteria were incubated with increasing concentrations of calprotectin, as previously described with modifications (25, 89, 110). Briefly, overnight cultures of *Y. pestis* carrying the pGEN-*luxCDABE* plasmid grown in BHI at 26 °C were diluted 1:50 in fresh BHI and grown for 4 h at 37 °C. Around 1×10^5 CFU were transferred to individual wells of a white 96-well plate (Greiner Bio-One) containing calprotectin in 38% BHI and 62% calprotectin buffer (20 mM Tris, pH 7.5, 100 mM NaCl, and 3 mM CaCl$_2$). Plates were incubated at 37 °C, and bacterial growth as a function of bioluminescence was measured using a Biotek Synergy HT plate reader (0.5 s read, sensitivity of 135), as previously described (63).

Statistics. All vertebrate animal experiments were repeated twice, and in vitro experiments were repeated three times to confirm reproducibility. Data are shown as the means ± SDs from three independent experiments, unless otherwise noted. *P* values were calculated using Student's *t* test, one-way ANOVA, or log-rank test, with appropriate post hoc testing as indicated. All statistics were completed using GraphPad Prism software.

Data Availability. All study data are included in the article and/or *SI Appendix*.

1. R. D. Perry, J. D. Fetherston, *Yersinia pestis*—Etiologic agent of plague. *Clin. Microbiol. Rev.* **10**, 35–66 (1997).
2. C. E. Demeure et al., *Yersinia pestis* and plague: An updated view on evolution, virulence determinants, immune subversion, vaccination, and diagnostics. *Genes Immun.* **20**, 357–370 (2019).
3. B. J. Hinnebusch, C. O. Jarrett, D. M. Bland, "Fleaing" the plague: Adaptations of *Yersinia pestis* to its insect vector that lead to transmission. *Annu. Rev. Microbiol.* **71**, 215–232 (2017).
4. R. J. Eisen et al., Early-phase transmission of *Yersinia pestis* by unblocked fleas as a mechanism explaining rapidly spreading plague epizootics. *Proc. Natl. Acad. Sci. U.S.A.* **103**, 15380–15385 (2006).
5. R. D. Pechous, V. Sivaraman, N. M. Stasulli, W. E. Goldman, Pneumonic plague: The darker side of *Yersinia pestis*. *Trends Microbiol.* **24**, 190–197 (2016).
6. W. W. Lathem, S. D. Crosby, V. L. Miller, W. E. Goldman, Progression of primary pneumonic plague: A mouse model of infection, pathology, and bacterial transcriptional activity. *Proc. Natl. Acad. Sci. U.S.A.* **102**, 17786–17791 (2005).

www.manaraa.com

7. T. V. Inglesby *et al.*, Working Group on Civilian Biodefense, Plague as a biological weapon: Medical and public health management. *JAMA* **283**, 2281–2290 (2000).

8. K. W. Becker, E. P. Skaar, Metal limitation and toxicity at the interface between host and pathogen. *FEMS Microbiol. Rev.* **38**, 1235–1249 (2014).

9. V. E. Diaz-Ochoa, S. Jellbauer, S. Klaus, M. Raffatellu, Transition metal ions at the crossroads of mucosal immunity and microbial pathogenesis. *Front. Cell. Infect. Microbiol.* **4**, 2 (2014).

10. C. A. Lopez, E. P. Skaar, The impact of dietary transition metals on host-bacterial interactions. *Cell Host Microbe* **23**, 737–748 (2018).

11. M. I. Hood, E. P. Skaar, Nutritional immunity: Transition metals at the pathogen-host interface. *Nat. Rev. Microbiol.* **10**, 525–537 (2012).

12. E. P. Skaar, M. Raffatellu, Metals in infectious diseases and nutritional immunity. *Metallomics* **7**, 926–928 (2015).

13. Z. R. Lonergan, E. P. Skaar, Nutrient zinc at the host-pathogen interface. *Trends Biochem. Sci.* **44**, 1041–1056 (2019).

14. L. D. Palmer, E. P. Skaar, Transition Metals and Virulence in Bacteria. *Annu. Rev. Genet.* **50**, 67–91 (2016).

15. V. Brinkmann *et al.*, Neutrophil extracellular traps kill bacteria. *Science* **303**, 1532–1535 (2004).

16. V. Brinkmann, A. Zychlinsky, Neutrophil extracellular traps: Is immunity the second function of chromatin? *J. Cell Biol.* **198**, 773–783 (2012).

17. C. F. Urban *et al.*, Neutrophil extracellular traps contain calprotectin, a cytosolic protein complex involved in host defense against *Candida albicans. PLoS Pathog.* **5**, e1000639 (2009).

18. K. Odink *et al.*, Two calcium-binding proteins in infiltrate macrophages of rheumatoid arthritis. *Nature* **330**, 80–82 (1987).

19. J. P. Zackular, W. J. Chazin, E. P. Skaar, Nutritional immunity: S100 proteins at the host-pathogen interface. *J. Biol. Chem.* **290**, 18991–18998 (2015).

20. I. P. Korndörfer, F. Brueckner, A. Skerra, The crystal structure of the human (S100A8/S100A9)2 heterotetramer, calprotectin, illustrates how conformational changes of interacting alpha-helices can determine specific association of two EF-hand proteins. *J. Mol. Biol.* **370**, 887–898 (2007).

21. J. A. Hayden, M. B. Brophy, L. S. Cunden, E. M. Nolan, High-affinity manganese coordination by human calprotectin is calcium-dependent and requires the histidine-rich site formed at the dimer interface. *J. Am. Chem. Soc.* **135**, 775–787 (2013).

22. M. B. Brophy, J. A. Hayden, E. M. Nolan, Calcium ion gradients modulate the zinc affinity and antibacterial activity of human calprotectin. *J. Am. Chem. Soc.* **134**, 18089–18100 (2012).

23. P. G. Sohnle, M. J. Hunter, B. Hahn, W. J. Chazin, Zinc-reversible antimicrobial activity of recombinant calprotectin (migration inhibitory factor-related proteins 8 and 14). *J. Infect. Dis.* **182**, 1272–1275 (2000).

24. J. L. Kelliher, T. E. Kehl-Fie, Competition for manganese at the host-pathogen interface. *Prog. Mol. Biol. Transl. Sci.* **142**, 1–25 (2016).

25. S. M. Damo *et al.*, Molecular basis for manganese sequestration by calprotectin and roles in the innate immune response to invading bacterial pathogens. *Proc. Natl. Acad. Sci. U.S.A.* **110**, 3841–3846 (2013).

26. T. E. Kehl-Fie *et al.*, Nutrient metal sequestration by calprotectin inhibits bacterial superoxide defense, enhancing neutrophil killing of *Staphylococcus aureus. Cell Host Microbe* **10**, 158–164 (2011).

27. J. A. Gaddy *et al.*, The host protein calprotectin modulates the *Helicobacter pylori* cag type IV secretion system via zinc sequestration. *PLoS Pathog.* **10**, e1004450 (2014).

28. M. I. Hood *et al.*, Identification of an *Acinetobacter baumannii* zinc acquisition system that facilitates resistance to calprotectin-mediated zinc sequestration. *PLoS Pathog.* **8**, e1003068 (2012).

29. C. A. Lopez *et al.*, The immune protein calprotectin impacts *Clostridioides difficile* metabolism through zinc limitation. *MBio* **10**, e02289–e02319 (2019).

30. B. D. Corbin *et al.*, Metal chelation and inhibition of bacterial growth in tissue abscesses. *Science* **319**, 962–965 (2008).

31. J. Z. Liu *et al.*, Zinc sequestration by the neutrophil protein calprotectin enhances *Salmonella* growth in the inflamed gut. *Cell Host Microbe* **11**, 227–239 (2012).

32. B. R. Wilson, A. R. Bogdan, M. Miyazawa, K. Hashimoto, Y. Tsuji, Siderophores in iron metabolism: From mechanism to therapy potential. *Trends Mol. Med.* **22**, 1077–1090 (2016).

33. A. Rakin, L. Schneider, O. Podladchikova, Hunger for iron: The alternative siderophore iron scavenging systems in highly virulent *Yersinia. Front. Cell. Infect. Microbiol.* **2**, 151 (2012).

34. R. D. Perry, J. D. Fetherston, Yersiniabactin iron uptake: Mechanisms and role in *Yersinia pestis* pathogenesis. *Microbes Infect.* **13**, 808–817 (2011).

35. R. Koczura, A. Kaznowski, Occurrence of the *Yersinia* high-pathogenicity island and iron uptake systems in clinical isolates of *Klebsiella pneumoniae. Microb. Pathog.* **35**, 197–202 (2003).

36. M. S. Lawlor, C. O'connor, V. L. Miller, Yersiniabactin is a virulence factor for *Klebsiella pneumoniae* during pulmonary infection. *Infect. Immun.* **75**, 1463–1472 (2007).

37. E. C. Garcia, A. R. Brumbaugh, H. L. T. Mobley, Redundancy and specificity of *Escherichia coli* iron acquisition systems during urinary tract infection. *Infect. Immun.* **79**, 1225–1235 (2011).

38. D. H. Wellawa, B. Allan, A. P. White, W. Köster, Iron-uptake systems of chicken-associated *Salmonella* serovars and their role in colonizing the avian host. *Microorganisms* **8**, 1203 (2020).

39. J. Mokracka, R. Koczura, A. Kaznowski, Yersiniabactin and other siderophores produced by clinical isolates of *Enterobacter spp.* and *Citrobacter spp. FEMS Immunol. Med. Microbiol.* **40**, 51–55 (2004).

40. R. D. Perry, P. B. Balbo, H. A. Jones, J. D. Fetherston, E. DeMoll, Yersiniabactin from *Yersinia pestis*: Biochemical characterization of the siderophore and its role in iron transport and regulation. *Microbiology (Reading)* **145**, 1181–1190 (1999).

41. S. W. Bearden, J. D. Fetherston, R. D. Perry, Genetic organization of the yersiniabactin biosynthetic region and construction of avirulent mutants in *Yersinia pestis. Infect. Immun.* **65**, 1659–1668 (1997).

42. M. C. Miller *et al.*, Reduced synthesis of the Ybt siderophore or production of aberrant Ybt-like molecules activates transcription of yersiniabactin genes in *Yersinia pestis. Microbiology (Reading)* **156**, 2226–2238 (2010).

43. M. C. Miller, S. Parkin, J. D. Fetherston, R. D. Perry, E. Demoll, Crystal structure of ferric-yersiniabactin, a virulence factor of *Yersinia pestis. J. Inorg. Biochem.* **100**, 1495–1500 (2006).

44. J. D. Fetherston, O. Kirillina, A. G. Bobrov, J. T. Paulley, R. D. Perry, The yersiniabactin transport system is critical for the pathogenesis of bubonic and pneumonic plague. *Infect. Immun.* **78**, 2045–2052 (2010).

45. J. D. Fetherston, J. W. Lillard Jr, R. D. Perry, Analysis of the pesticin receptor from *Yersinia pestis*: Role in iron-deficient growth and possible regulation by its siderophore. *J. Bacteriol.* **177**, 1824–1833 (1995).

46. J. D. Fetherston, V. J. Bertolino, R. D. Perry, YbtP and YbtQ: Two ABC transporters required for iron uptake in Yersinia pestis. *Mol. Microbiol.* **32**, 289–299 (1999).

47. A. R. Brumbaugh *et al.*, Blocking yersiniabactin import attenuates extraintestinal pathogenic *Escherichia coli* in cystitis and pyelonephritis and represents a novel target to prevent urinary tract infection. *Infect. Immun.* **83**, 1443–1450 (2015).

48. V. Hancock, L. Ferrières, P. Klemm, The ferric yersiniabactin uptake receptor FyuA is required for efficient biofilm formation by urinary tract infectious *Escherichia coli* in human urine. *Microbiology (Reading)* **154**, 167–175 (2008).

49. E.-I. Koh *et al.*, Metal selectivity by the virulence-associated yersiniabactin metallophore system. *Metallomics* **7**, 1011–1022 (2015).

50. E.-I. Koh, A. E. Robinson, N. Bandara, B. E. Rogers, J. P. Henderson, Copper import in *Escherichia coli* by the yersiniabactin metallophore system. *Nat. Chem. Biol.* **13**, 1016–1021 (2017).

51. A. E. Robinson, J. R. Heffernan, J. P. Henderson, The iron hand of uropathogenic *Escherichia coli*: The role of transition metal control in virulence. *Future Microbiol.* **13**, 745–756 (2018).

52. H. Zhi *et al.*, Siderophore-mediated zinc acquisition enhances enterobacterial colonization of the inflamed gut. *bioRxiv* [Preprint] (2020). https://www.biorxiv.org/content/10.1101/2020.07.20.212498v1. Accessed 28 February 2021.

53. D. C. Desrosiers *et al.*, Znu is the predominant zinc importer in *Yersinia pestis* during in vitro growth but is not essential for virulence. *Infect. Immun.* **78**, 5163–5177 (2010).

54. A. G. Bobrov *et al.*, The *Yersinia pestis* siderophore, yersiniabactin, and the ZnuABC system both contribute to zinc acquisition and the development of lethal septicaemic plague in mice. *Mol. Microbiol.* **93**, 759–775 (2014).

55. A. G. Bobrov *et al.*, Zinc transporters YbtX and ZnuABC are required for the virulence of *Yersinia pestis* in bubonic and pneumonic plague in mice. *Metallomics* **9**, 757–772 (2017).

56. F. W. Huang, J. L. Pinkus, G. S. Pinkus, M. D. Fleming, N. C. Andrews, A mouse model of juvenile hemochromatosis. *J. Clin. Invest.* **115**, 2187–2191 (2005).

57. L. E. Quenee *et al.*, Hereditary hemochromatosis restores the virulence of plague vaccine strains. *J. Infect. Dis.* **206**, 1050–1058 (2012).

58. R. Rebeil *et al.*, Induction of the *Yersinia pestis* PhoP-PhoQ regulatory system in the flea and its role in producing a transmissible infection. *J. Bacteriol.* **195**, 1920–1930 (2013).

59. A. Lemon, A. Silva-Rohwer, J. Sagawa, V. Vadyvaloo, Co-infection assay to determine *Yersinia pestis* competitive fitness in fleas. *Methods Mol. Biol.* **2010**, 153–166 (2019).

60. L. C. Martínez-Chavarría *et al.*, Putative horizontally acquired genes, highly transcribed during *Yersinia pestis* flea infection, are induced by hyperosmotic stress and function in aromatic amino acid metabolism. *J. Bacteriol.* **202**, e00733-19 (2020).

61. J. E. Comer *et al.*, Transcriptomic and innate immune responses to *Yersinia pestis* in the lymph node during bubonic plague. *Infect. Immun.* **78**, 5086–5098 (2010).

62. M. A. Bachman *et al.*, *Klebsiella pneumoniae* yersiniabactin promotes respiratory tract infection through evasion of lipocalin 2. *Infect. Immun.* **79**, 3309–3316 (2011).

63. Y. Sun, M. G. Connor, J. M. Pennington, M. B. Lawrenz, Development of bioluminescent bioreporters for in vitro and in vivo tracking of *Yersinia pestis. PLoS One* **7**, e47123 (2012).

64. D. E. Brodersen, J. Nyborg, M. Kjeldgaard, Zinc-binding site of an S100 protein revealed. Two crystal structures of Ca2+-bound human psoriasin (S100A7) in the Zn^{2+}-loaded and Zn^{2+}-free states. *Biochemistry* **38**, 1695–1704 (1999).

65. O. V. Moroz, E. V. Blagova, A. J. Wilkinson, K. S. Wilson, I. B. Bronstein, The crystal structures of human S100A12 in apo form and in complex with zinc: New insights into S100A12 oligomerisation. *J. Mol. Biol.* **391**, 536–551 (2009).

66. M. P. Manitz *et al.*, Loss of S100A9 (MRP14) results in reduced interleukin-8-induced CD11b surface expression, a polarized microfilament system, and diminished responsiveness to chemoattractants in vitro. *Mol. Cell. Biol.* **23**, 1034–1043 (2003).

67. J. Kramer, Ö. Özkaya, R. Kümmerli, Bacterial siderophores in community and host interactions. *Nat. Rev. Microbiol.* **18**, 152–163 (2020).

Price *et al.*
Yersiniabactin contributes to overcoming zinc restriction during *Yersinia pestis* infection of mammalian and insect hosts

PNAS | 9 of 10
https://doi.org/10.1073/pnas.2104073118

www.manaraa.com

68. N. Moscatello *et al.*, Continuous removal of copper, magnesium, and nickel from industrial wastewater utilizing the natural product yersiniabactin immobilized within a packed-bed column. *Chem. Eng. J.* **343**, 173–179 (2018).

69. K. S. Chaturvedi, C. S. Hung, J. R. Crowley, A. E. Stapleton, J. P. Henderson, The siderophore yersiniabactin binds copper to protect pathogens during infection. *Nat. Chem. Biol.* **8**, 731–736 (2012).

70. H. Drechsel *et al.*, Structure elucidation of yersiniabactin, a siderophore from highly virulent *Yersinia* strains. *Liebigs Ann.* **1995**, 1727–1733 (1995).

71. B. A. Pfeifer, C. C. Wang, C. T. Walsh, C. Khosla, Biosynthesis of Yersiniabactin, a complex polyketide-nonribosomal peptide, using *Escherichia coli* as a heterologous host. *Appl. Environ. Microbiol.* **69**, 6698–6702 (2003).

72. L. Wisgrill *et al.*, Outbreak of yersiniabactin-producing *Klebsiella pneumoniae* in a neonatal intensive care unit. *Pediatr. Infect. Dis. J.* **38**, 638–642 (2019).

73. C. Shankar *et al.*, Whole genome analysis of hypervirulent *Klebsiella pneumoniae* isolates from community and hospital acquired bloodstream infection. *BMC Microbiol.* **18**, 6 (2018).

74. P. A. Remya, M. Shanthi, U. Sekar, Characterisation of virulence genes associated with pathogenicity in *Klebsiella pneumoniae*. *Indian J. Med. Microbiol.* **37**, 210–218 (2019).

75. S. E. Heiden *et al.*, A *Klebsiella pneumoniae* ST307 outbreak clone from Germany demonstrates features of extensive drug resistance, hypermucoviscosity, and enhanced iron acquisition. *Genome Med.* **12**, 113 (2020).

76. D. L. Geiser, J. J. Winzerling, Insect transferrins: Multifunctional proteins. *Biochim. Biophys. Acta* **1820**, 437–451 (2012).

77. I. Iatsenko, A. Marra, J.-P. Boquete, J. Peña, B. Lemaitre, Iron sequestration by transferrin 1 mediates nutritional immunity in *Drosophila melanogaster*. *Proc. Natl. Acad. Sci. U.S.A.* **117**, 7317–7325 (2020).

78. B. J. Hinnebusch, R. D. Perry, T. G. Schwan, Role of the *Yersinia pestis* hemin storage (hms) locus in the transmission of plague by fleas. *Science* **273**, 367–370 (1996).

79. F. Sebbane, C. Jarrett, D. Gardner, D. Long, B. J. Hinnebusch, Role of the *Yersinia pestis* yersiniabactin iron acquisition system in the incidence of flea-borne plague. *PLoS One* **5**, e14379 (2010).

80. T. P. Driscoll *et al.*, A chromosome-level assembly of the cat flea genome uncovers rampant gene duplication and genome size plasticity. *BMC Biol.* **18**, 70 (2020).

81. T. Wang *et al.*, Type VI secretion system transports Zn^{2+} to combat multiple stresses and host immunity. *PLoS Pathog.* **11**, e1005020 (2015).

82. R. Cai *et al.*, The transcriptional regulator Zur regulates the expression of ZnuABC and T6SS4 in response to stresses in *Yersinia pseudotuberculosis*. *Microbiol. Res.* **249**, 126787 (2021).

83. T. Wang *et al.*, ZntR positively regulates T6SS4 expression in *Yersinia pseudotuberculosis*. *J. Microbiol.* **55**, 448–456 (2017).

84. Y. Li *et al.*, Characterization of Zur-dependent genes and direct Zur targets in *Yersinia pestis*. *BMC Microbiol.* **9**, 128 (2009).

85. I. Chouikha, D. E. Sturdevant, C. Jarrett, Y.-C. Sun, B. J. Hinnebusch, Differential gene expression patterns of *Yersinia pestis* and *Yersinia pseudotuberculosis* during infection and biofilm formation in the flea digestive tract. *mSystems* **4**, e00217–e00218 (2019).

86. T. E. Kehl-Fie *et al.*, MntABC and MntH contribute to systemic *Staphylococcus aureus* infection by competing with calprotectin for nutrient manganese. *Infect. Immun.* **81**, 3395–3405 (2013).

87. A. M. Nuss *et al.*, Transcriptomic profiling of *Yersinia pseudotuberculosis* reveals reprogramming of the Crp regulon by temperature and uncovers Crp as a master regulator of small RNAs. *PLoS Genet.* **11**, e1005087 (2015).

88. L. R. Burcham *et al.*, Identification of zinc-dependent mechanisms used by group B *Streptococcus* to overcome calprotectin-mediated stress. *MBio* **11**, e02302–e02320 (2020).

89. K. P. Grim *et al.*, The metallophore staphylopine enables *Staphylococcus aureus* to compete with the host for zinc and overcome nutritional immunity. *MBio* **8**, e01281–e01317 (2017).

90. R. D. Perry *et al.*, Manganese transporters Yfe and MntH are Fur-regulated and important for the virulence of *Yersinia pestis*. *Microbiology (Reading)* **158**, 804–815 (2012).

91. K. Cao *et al.*, The mechanism of iron-compensation for manganese deficiency of *Streptococcus pneumoniae*. *J. Proteomics* **184**, 62–70 (2018).

92. T. M. Staggs, R. D. Perry, Identification and cloning of a fur regulatory gene in *Yersinia pestis*. *J. Bacteriol.* **173**, 417–425 (1991).

93. J. Edgeworth, M. Gorman, R. Bennett, P. Freemont, N. Hogg, Identification of p8,14 as a highly abundant heterodimeric calcium binding protein complex of myeloid cells. *J. Biol. Chem.* **266**, 7706–7713 (1991).

94. P. A. Clohessy, B. E. Golden, Calprotectin-mediated zinc chelation as a biostatic mechanism in host defence. *Scand. J. Immunol.* **42**, 551–556 (1995).

95. H. L. Clark *et al.*, Zinc and manganese chelation by neutrophil S100A8/A9 (calprotectin) limits extracellular *Aspergillus fumigatus* hyphal growth and corneal infection. *J. Immunol.* **196**, 336–344 (2016).

96. J. G. Shannon, B. J. Hinnebusch, Antibody opsonization enhances early interactions between *Yersinia pestis* and neutrophils in the skin and draining lymph node in a mouse model of bubonic plague. *Infect. Immun.* **89**, e00061-20 (2020).

97. R. J. Gonzalez, M. C. Lane, N. J. Wagner, E. H. Weening, V. L. Miller, Dissemination of a highly virulent pathogen: Tracking the early events that define infection. *PLoS Pathog.* **11**, e1004587 (2015).

98. Y. Vagima *et al.*, Circumventing *Y. pestis* virulence by early recruitment of neutrophils to the lungs during pneumonic plague. *PLoS Pathog.* **11**, e1004893 (2015).

99. A. N. Besold *et al.*, Antimicrobial action of calprotectin that does not involve metal withholding. *Metallomics* **10**, 1728–1742 (2018).

100. J. Behnsen *et al.*, The cytokine IL-22 promotes pathogen colonization by suppressing related commensal bacteria. *Immunity* **40**, 262–273 (2014).

101. J. D. Fetherston, P. Schuetze, R. D. Perry, Loss of the pigmentation phenotype in *Yersinia pestis* is due to the spontaneous deletion of 102 kb of chromosomal DNA which is flanked by a repetitive element. *Mol. Microbiol.* **6**, 2693–2704 (1992).

102. J. J. Merriam, R. Mathur, R. Maxfield-Boumil, R. R. Isberg, Analysis of the *Legionella pneumophila fliI* gene: Intracellular growth of a defined mutant defective for flagellum biosynthesis. *Infect. Immun.* **65**, 2497–2501 (1997).

103. S. Gong, S. W. Bearden, V. A. Geoffroy, J. D. Fetherston, R. D. Perry, Characterization of the *Yersinia pestis* Yfu ABC inorganic iron transport system. *Infect. Immun.* **69**, 2829–2837 (2001).

104. M. C. Lane, C. J. Alteri, S. N. Smith, H. L. Mobley, Expression of flagella is coincident with uropathogenic *Escherichia coli* ascension to the upper urinary tract. *Proc. Natl. Acad. Sci. U.S.A.* **104**, 16669–16674 (2007).

105. G. Dinc, J. M. Pennington, E. S. Yolcu, M. B. Lawrenz, H. Shirwan, Improving the Th1 cellular efficacy of the lead *Yersinia pestis* rF1-V subunit vaccine using SA-4-1BBL as a novel adjuvant. *Vaccine* **32**, 5035–5040 (2014).

106. W. Bowen *et al.*, Robust Th1 cellular and humoral responses generated by the *Yersinia pestis* rF1-V subunit vaccine formulated to contain an agonist of the CD137 pathway do not translate into increased protection against pneumonic plague. *Vaccine* **37**, 5708–5716 (2019).

107. National Research Council, *Guide for the Care and Use of Laboratory Animals* (National Academies Press, Washington, DC, ed. 8, 2011).

108. S. A. Handley, P. H. Dube, V. L. Miller, Histamine signaling through the H(2) receptor in the Peyer's patch is important for controlling *Yersinia enterocolitica* infection. *Proc. Natl. Acad. Sci. U.S.A.* **103**, 9268–9273 (2006).

109. R. D. Pechous, Intranasal inoculation of mice with *Yersinia pestis* and processing of pulmonary tissue for analysis. *Methods Mol. Biol.* **2010**, 17–28 (2019).

110. J. N. Radin, J. L. Kelliher, P. K. Párraga Solórzano, T. E. Kehl-Fie, The two-component system ArlRS and alterations in metabolism enable *Staphylococcus aureus* to resist calprotectin-induced manganese starvation. *PLoS Pathog.* **12**, e1006040 (2016).

Price et al.
Yersiniabactin contributes to overcoming zinc restriction during *Yersinia pestis* infection of mammals and insects